

GROWTH AND CHARACTERIZATION OF PURE AND Ni^{2+} DOPED GLYCINE SODIUM SULFATE CRYSTALS

A.Karolin¹, K.Jayakumari², C.K.Mahadevan³

^{1,3}Physics Research Centre, S.T.Hindu College, Nagercoil-629002, Tamilnadu, India

²Department of Physics, SreeAyyappa College for Women, Chunkankadai-629807, Tamilnadu, India
karolin_augustin@yahoo.com, jaya_shrik@yahoo.co.in, mahadevan58@yahoo.co.in

Abstract

Single crystals of glycine sodium sulfate (GSS), a new semi-organic nonlinear optical (NLO) material, have been grown by the free evaporation method and characterized chemically, structurally, thermally, optically and mechanically. Effect of Ni^{2+} addition as an impurity on the properties of GSS has also been investigated. X-ray diffraction analysis indicates the crystal system as monoclinic. The functional groups have been identified using Fourier transform infrared spectral analysis. The crystals are found to be thermally stable up to 250°C. The UV-Vis-NIR spectral analysis shows that these crystals have their cut off wavelengths around 250nm. Second harmonic generation (SHG) measurement shows the NLO property. Micro hardness measurement indicates that GSS comes under soft material category. The Ni^{2+} addition is found to increase the optical transparency and micro hardness whereas it decreases the second harmonic generation efficiency.

Keywords: Crystal growth, Thermal properties, Mechanical properties, Optical properties, X-ray diffraction

1. INTRODUCTION

Nonlinear optical (NLO) materials for optical second harmonic generation (SHG) have received much attention owing to their practical application in the domain of optoelectronics and photonics. Crystalline semi-organic salts of amino acids have recently attracted considerable interest among researchers. The amino acid group materials have been mixed with inorganic salts to form adducts or complexes in order to improve their mechanical, thermal and NLO properties [1-3].

Glycine is the simplest amino acid and is found to exist in three polymorphic crystalline forms, namely, α , β and γ . Alpha glycine, the basic of all amino acids having zwitterionic character, has been employed to synthesize many organic and semi-organic materials (may be in the form of adducts or complexes) exhibiting dielectric, ferroelectric, NLO and light sensing behavior [4, 5]. Some complexes of glycine with inorganic salts have already been reported to be promising materials for SHG: glycine sodium nitrate [6], glycine silver nitrate [7], glycine hydrogen nitrate [8], glycine hydrogen phosphate [2], glycine potassium sulfate [9], glycine lithium sulfate [10], glycine zinc sulfate [11], glycine zinc chloride [12], diglycine manganese chloride [13], triglycinefluoroberyllate [14], etc.

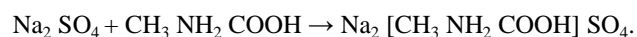
It is a known fact and it is generally understood that materials with wide range of optical properties are required for practical applications. In order to satisfy this requirement it is necessary

either to discover new materials or to modify the existing materials. In an attempt to discover new crystalline materials for industrial applications, in the present study, we have made an attempt to combine α -glycine with sodium sulfate to form glycine sodium sulfate (GSS) single crystal. Also, we have investigated the effect of Ni^{2+} (by adding nickel sulfate to sodium sulfate in different molar ratios) as an impurity on the physical properties of GSS single crystals. The results obtained are reported herein and discussed.

2. EXPERIMENTAL

2.1. Crystal Growth

Analytical reagent (AR) grade α -glycine, sodium sulfate (Na_2SO_4) and nickel sulfate heptahydrate ($\text{NiSO}_4 \cdot 7\text{H}_2\text{O}$) were used along with double distilled water (as a solvent) for the growth of single crystals by the free evaporation method. Sodium sulfate and α -glycine mixed in 1:1 molar ratio were dissolved in double distilled water and stirred for two hours to obtain a homogeneous solution. The solution was filtered and kept in a dust free environment. Transparent and colorless single crystals of glycine sodium sulfate (GSS) were formed at room temperature in a period of about 30 days as per the reaction



GSS was added with $\text{NiSO}_4 \cdot 7\text{H}_2\text{O}$ in five different molar ratios, viz. 1:0.002, 1:0.004, 1:0.006, 1:0.008, and 1:0.010 and the five different Ni^{2+} doped GSS crystals were grown in a

period of about 30 days similarly under identical conditions with the pure GSS crystal growth.

2.2. Characterizations

Density was measured by the flotation method [15, 16] within an accuracy of $\pm 0.008 \text{ g/cm}^3$. Carbon tetrachloride of density 1.594 g/cm^3 and bromoform of density 2.890 g/cm^3 were respectively the rarer and denser liquids used.

Atomic absorption spectroscopic (ASS) measurements were carried out using an atomic absorption analyzer (Model AA-6300) to determine the metal atom content of the impurity added crystals grown.

Single crystal X-ray diffraction (SXRD) analysis was performed and lattice parameters were determined for the pure GSS crystal using a BRUKER KAPPA APEX II diffractometer with CuK_α radiation ($\lambda = 1.54056 \text{ \AA}$). X-ray powder diffraction (PXRD) analysis was carried out for all the six crystals grown using an automated X-ray powder diffractometer (PANalytical) in the 2θ range $10-70^\circ$ with CuK_α radiation ($\lambda = 1.54056 \text{ \AA}$). The reflection data were indexed following the procedures of Lipson and Steeple [17].

Fourier transform infrared (FTIR) spectra were recorded by the KBr pellet method for all the six crystals grown in the wavenumber range $400-4000 \text{ cm}^{-1}$ by using a SHIMADZU spectrometer.

Thermogravimetric analysis (TGA) was carried out for the pure GSS crystal using a Perkin Elmer thermal analyzer at a heating rate of 10°C/min in the nitrogen atmosphere heated from $40-950^\circ\text{C}$ to understand the thermal stability of the crystals.

The UV-Vis-NIR absorption spectra were recorded in the wavelength range $190-1100 \text{ nm}$ for all the six crystals grown by using a Lambda-35 spectrophotometer.

The NLO property of the grown crystals was tested by passing the output of Nd:YAG Quanta ray laser (with fundamental radiation of wavelength 1064 nm) through the crystalline powder sample (Kurtz and Perry method [18]). The SHG output from the sample was compared with that from KDP.

Vickers hardness measurements were carried out on all the grown crystals by making indentations on the large area faces using a SHIMADZU HMV2 micro hardness tester.

3. RESULTS AND DISCUSSION

3.1. Densities, Lattice Parameters and Chemical Composition

The single crystals grown in the present study are represented as: Pure GSS \rightarrow the undoped GSS crystal; GN1, GN2, GN3,

GN4 and GN5 \rightarrow 0.2, 0.4, 0.6, 0.8 and 1.0 mol% Ni^{2+} doped GSS crystals respectively.

Fig-1 shows a photograph of the pure and Ni^{2+} added single crystals grown in the present study. The grown crystals are transparent and colorless. Morphology of the Ni^{2+} doped GSS crystals is observed to be similar to that of the pure GSS crystal. Also, significant coloration has not been observed due to Ni^{2+} doping.

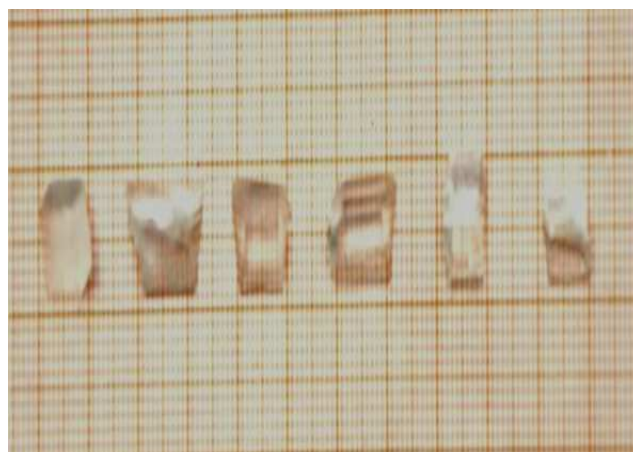


Fig-1: Photograph showing the pure and Ni^{2+} doped GSS crystals
(From left: Pure GSS, GN1, GN2, GN3, GN4 and GN5)

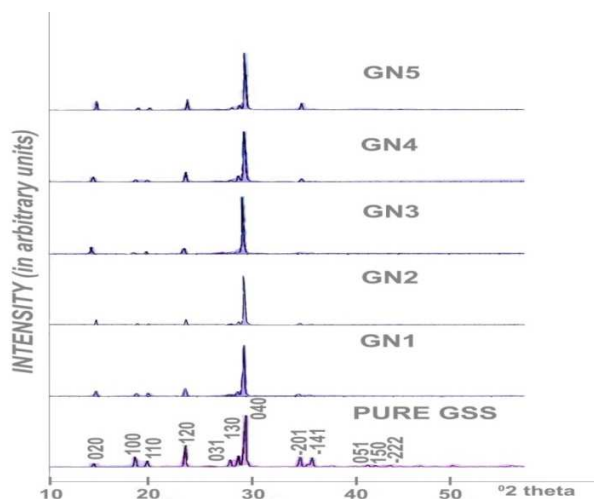
The densities and metal atom (Ni) contents observed in the present study are provided in Table-1. The observed metal atom contents confirm the presence of Ni atom in the doped GSS crystals. The density is found to increase with the increase in impurity (dopant) concentration. This may be due to the incorporation of Ni atoms in the interstitial positions and/or due to the replacement of Na atoms by the Ni atoms in the host (GSS) crystal matrix. If the dopant atoms occupy the crystal matrix, mass increases (atomic weight of Ni is more than that of Na) and hence density increases. The density variation shows clearly that the dopant atoms have entered proportionately with the GSS crystal matrix nearly as per the dopant concentration considered in the solution used for the growth of single crystals.

Table-1: Densities, Ni atom contents and lattice parameters for the pure and Ni²⁺ doped GSS crystals. The e.s.d.s are in parenthesis.

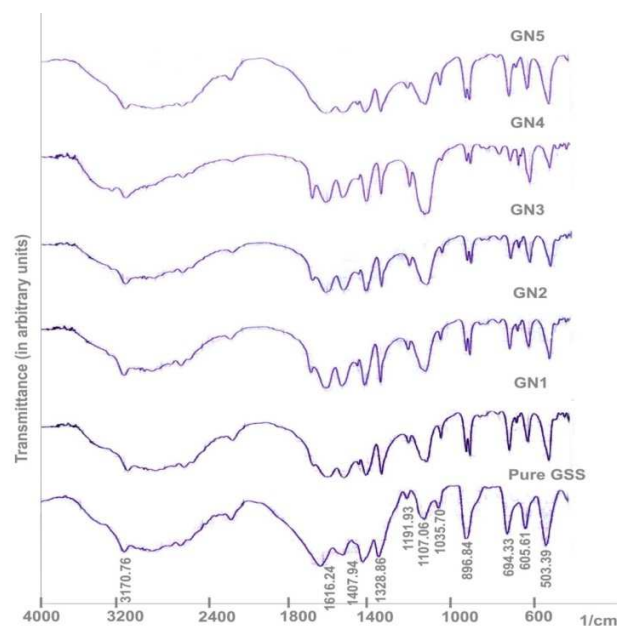
Crystal	Density (g/cm ³)	Ni content (ppm)	Lattice parameters				
			a (Å)	b (Å)	c (Å)	β(°)	Volume(Å ³)
Pure GSS	1.704	-	5.1000(2)	11.9400(3)	5.4600(2)	111.75(2)	308.8(1)
GN1	1.710	110	5.0726(3)	12.0000(4)	5.5062(3)	112.12(2)	310.5(1)
GN2	1.723	136	5.1238(1)	11.9850(2)	5.4849(3)	113.98(2)	307.7(2)
GN3	1.733	142	5.0939(2)	12.0600(1)	5.4847(1)	111.75(2)	312.9(1)
GN4	1.740	173	5.0848(4)	12.0140(1)	5.5155(1)	111.90(1)	312.6(2)
GN5	1.758	202	5.0900(1)	11.9901(1)	5.4700(2)	111.69(1)	310.2(1)

The lattice parameters of pure and Ni²⁺ doped GSS crystals obtained through SXRD analysis are presented in Table-1. The study reveals that pure and Ni²⁺ doped GSS crystallize in the monoclinic system and belongs to the P2₁ space group. The observed difference in the lattice volumes is very small to have any lattice distortion in the GSS crystal due to doping. This confirms that the dopant atoms have entered into the GSS crystal matrix but not distorted the regular structure of the GSS crystal. Further, the ionic radius of Na⁺ is 0.95 Å and that of Ni²⁺ is 0.72 Å. So, replacement of Na⁺ by Ni²⁺ is not expected to distort the crystal structure significantly. In addition the lattice volume does not vary systematically with the dopant concentration indicating the dopant concentrations considered in the present study are significantly small to create any lattice distortion in the GSS crystal.

The recorded PXRD patterns of the grown crystals are shown in Fig-2. Appearance of sharp and strong peaks confirms the crystalline nature of the samples. The diffraction peaks were indexed for the monoclinic system.

**Fig-2:** The powder X-ray diffraction patterns for pure and Ni²⁺ added GSS crystals

The FTIR spectra of pure and doped GSS crystals are shown in Fig-3. Significant difference could not be observed for the doped crystals due to the lower level of dopant concentration. The peaks observed at nearly 503, 698, 1408 and 1609 cm⁻¹ can be assigned to the carboxylate (COO⁻) group of the glycine part. The peaks for the ammonium (NH₃⁺) group of glycine part are observed at nearly 1111 and 3171 cm⁻¹. From the presence of carboxylate and ammonium ions it may be concluded that glycine molecules exist in zwitterionic form in GSS crystals. The peaks observed at nearly 893 and 1034 cm⁻¹ can be assigned to the CCN group. The peaks observed at nearly 1333 cm⁻¹ correspond to the CH₂ group. Observation of peaks at nearly 606 and 750 cm⁻¹ can be assigned to the SO₄²⁻ group. A less intense peak observed at nearly 2122 cm⁻¹ may be due to the combination bond. Thus, with the help of available data on the vibrational frequencies of amino acids [19] all the molecular groups present in the GSS crystals could be identified.

**Fig-3:** The FTIR spectra for pure and Ni²⁺ doped GSS crystals

In effect, the results obtained through ASS, SXRD, PXRD and FTIR spectral analyses confirm the materials (pure and Ni²⁺ doped GSS) of the crystals grown in the present study.

3.2. Thermal, Optical and Mechanical Properties

The TGA pattern obtained for the pure GSS crystal is shown in Fig-4. It can be noticed that there is no loss of weight of the crystal sample up to around 250°C showing the absence of any adsorbed water molecule in the GSS crystal. The weight loss around 250°C represents the decomposition of the glycine from the GSS crystal. The gradual weight loss after this temperature can be attributed to the sublimation of sodium sulfate. Hence, it can be understood that the GSS crystal is stable up to 250°C. This ensures suitability of this material for possible application in lasers where the crystals are required to withstand high temperatures.

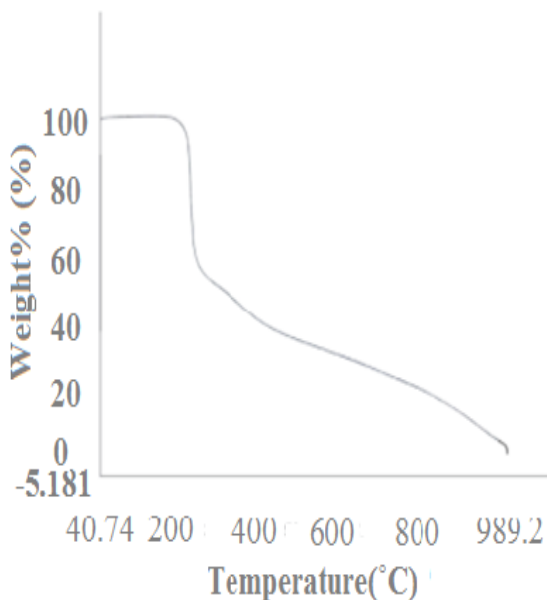


Fig-4: TGA pattern for the pure GSS crystal

The UV-Vis-NIR absorption spectra observed for the pure and Ni²⁺ doped GSS crystals are shown in Fig-5. It can be noticed that doping with Ni²⁺ increased the transparency in the UV range. The absorption edges observed are provided in Table-2. Efficient nonlinear optical (NLO) crystals have optical transparency lower cut-off wavelengths between 200 and 400nm [20]. This indicates that the crystals grown in the present study can be considered as promising NLO crystals. The SHG efficiency decreases as the dopant concentration increases (see Table-2).

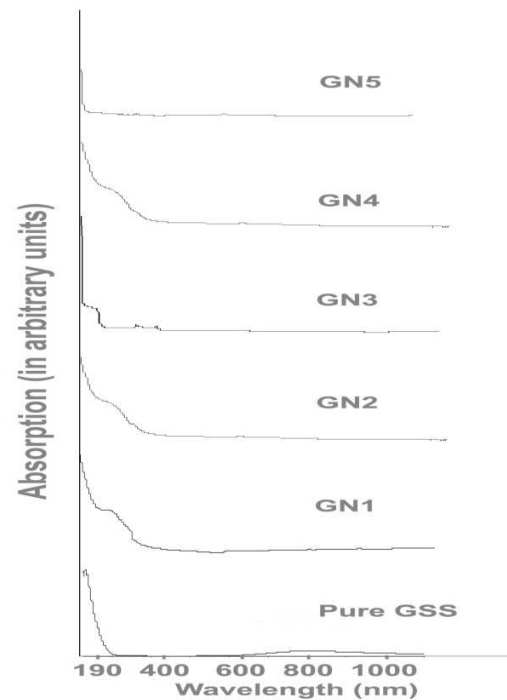


Fig-5: UV-Vis-NIR spectra for the pure and Ni²⁺ doped GSS crystals

Table-2: Optical absorption edges, SHG efficiencies and work hardening coefficients (n) for the pure and Ni²⁺ doped GSS crystals.

Crystal	Absorption edge (nm)	SHG efficiency (in KDP unit)	n
Pure GSS	296	0.43	7.52
GN1	243	0.31	5.06
GN2	248	0.28	5.63
GN3	244	0.25	6.25
GN4	244	0.22	3.95
GN5	249	0.18	3.07

The hardness behavior and log P versus log d plots for the pure and Ni²⁺ doped GSS crystals are shown in Figure 6. P is the load applied and d is the diagonal length of the indentation made on the crystal surface. The Vickers hardness number is defined as

$$H_v = 1.8544 P/d^2 \text{ kg/mm}^2 \dots\dots\dots(4)$$

It can be noticed that the H_v value increases with increasing load ((see Fig-6(a)). The H_v value increases up to a load of 100g, above which cracks start developing, which may be due

to the release of internal stress generation with indentation. The work hardening exponents (coefficients, n) estimated from the slopes of the best-fitted straight lines of $\log P$ versus $\log d$ curves (see Fig-6 (b)) are provided in Table-2.

The Meyer's law [21] is expressed as,

$$P = K_1 d^n \dots \dots \dots (5)$$

where K_1 is the material constant. Combining equations (4) and (5), we have

$$H_v = 1.8544 K_1 d^{n-2}$$

$$\text{or } H_v = 1.8544 K_1^{(1+2/n)} P^{(1-2/n)}$$

$$\text{or } H_v = b P^{(n-2)/n} \dots \dots \dots (6)$$

where $b = 1.8544 K_1^{(1+2/n)}$, a new constant. The above expression shows that H_v should increase with the load if $n > 2$. This is in good agreement with the experimental data observed in the present study and this confirms the normal indentation size effect (ISE). Phenomenon of dependence of micro hardness of a solid on the applied load at low level of testing load is known as indentation size effect [22].

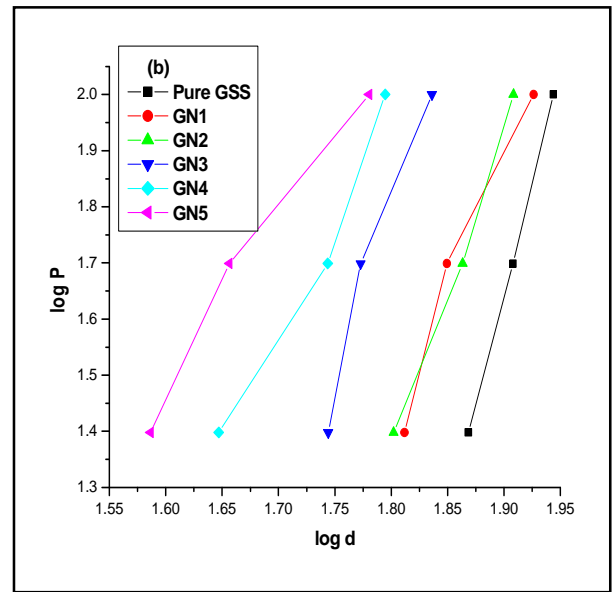
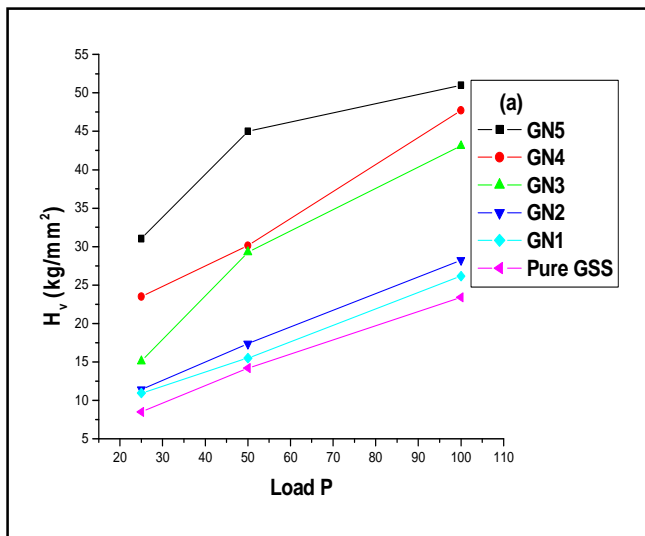


Fig-6: Hardness behavior (a) and $\log P$ versus $\log d$ plots (b) for the pure and Ni^{2+} doped GSS crystals

According to Onitsch [23] and Hanneman [24] ' n ' should lie between 1.0 and 1.6 for hard materials and above 1.6 for soft ones. Thus, the pure and Ni^{2+} doped GSS crystals belong to soft materials category. Hence, the experimental results observed in the present study follow the normal ISE trend.

CONCLUSIONS

Pure and Ni^{2+} doped glycine sodium sulfate (GSS) single crystals have been successfully grown by the free evaporation method and characterized. They belong to monoclinic system. X-ray diffraction measurements indicate no lattice distortion due to Ni^{2+} doping. The GSS crystal is found to be thermally stable up to 250°C and mechanically soft. NLO property is confirmed by Kurtz and Perry technique. Tuning the optical and mechanical properties could be understood as possible by Ni^{2+} doping.

REFERENCES

- [1]. M.N. Bhat and S.M. Dharmaprakash, J. Cryst. Growth 235 (2002) 511-516.
- [2]. A. Deepthy and H.L. Bhat, J. Cryst. Growth 226 (2001) 287-293.
- [3]. R. Rajasekaran, P.M. Ushashree, R. Jayavel and P. Ramasamy, J. Cryst. Growth 229 (2001) 563-567.
- [4]. R. Pepinsky, Y. Okaya, D.P. Eastman and T. Mitsui, Phys. Rev. 107 (1957) 1538.
- [5]. M.M. Khandpekar and S.P. Pati, J. Opt. Commun. 283 (2010) 2700-2704.
- [6]. M.N. Bhat and S.M. Dharmaprakash, J. Cryst. Growth 236 (2002) 376-380.

- [7]. J.K. Mohan Rao and M.A. Vishwamitra, ActaCrystallogr. B 28 (1972) 1484.
- [8]. S.A. Martin Britto and S. Natarajan, Mater. Lett. 62 (2008) 2633-2636.
- [9]. Ra. Shanmugavadivu, G. Ravi and A. Nixon Azariah, J. Phys. and Chem. Solids 67 (2006) 1858-1861.
- [10]. M.R. Suresh Kumar, H.J. Ravindra and S.M. Dharmaparakash, J. Cryst. Growth 306 (2007) 361-365.
- [11]. T. Balakrishnan and K. Ramamurthi, Spectrochim. Acta Part A 68 (2007) 360-363.
- [12]. T. Balakrishnan and K. Ramamurthi, Mater. Lett. 62 (2008) 65-68.
- [13]. R. Pepinsky, K. Vedam and Y. Okaya, Phys. Rev. 110 (1958) 1309-1311.
- [14]. S. Hoshino, T. Mitsui, F. Jona and R. Pepinsky, Phys. Rev. 107(1957) 1255-1258.
- [15]. T.H. Freeda and C.K. Mahadevan, Bull. Mater. Sci. 23 (2000) 335-340.
- [16]. K. Jayakumari and C.K. Mahadevan, J. Phys. Chem. Solids 66 (2005) 1705-1713.
- [17]. H. Lipson and H. Steeple Interpretation of X-ray power Diffraction Patterns, MacMillan, New York, 1970.
- [18]. S.K. Kurtz and T.T. Perry, J. Appl. Crystallography 9 (1968) 3798-3813.
- [19]. R.S. Krishnan, K. Sankaranarayanan and K. Krishnan, J. Indian Inst. Sci. 55 (1973) 313.
- [20]. U. Le. Fur, R. Masse, M.Z. Cherkaoui and J.K. Nicoud, Z. Kristallogr. 210 (1995) 856.
- [21]. E. Meyer, Z. Ver. Dtsch. Ing. 52 (1908) 645.
- [22]. S.Karan and S.P. Sen Gupta, Mater.Sci.Eng. A398 (2005) 198-203.
- [23]. E.M. Onitsch, Mikroskopie 2 (1947) 131.
- [24]. M. Hanneman, Metall. Manchu. 23 (1941) 135.